Research Article

Aljawhara H. Almuqrin, Heba Jamal ALasali, M. I. Sayyed*, and K. G. Mahmoud

Preparation and experimental estimation of radiation shielding properties of novel epoxy reinforced with Sb_2O_3 and PbO

https://doi.org/10.1515/epoly-2023-0019
received March 08, 2023; accepted April 06, 2023

Abstract: The present work aims to fabricate new inexpensive epoxy-based composites with a concentration described by the formula $(90 - x)$epoxy + $10Sb_2O_3$ + xPbO, where x = 5, 10, 15, and 20 wt%. The impacts of the substitution of epoxy by PbO on the composite density and radiation shielding properties of the fabricated composites were studied. The density of the fabricated composites varied between 1.30 and 1.49 g·cm^{-3}, enriching the PbO concentration. Utilizing the narrow beam transmission method, the linear attenuation coefficient (LAC) of the fabricated composites was measured using the NaI (Tl) detector as well as radioactive sources Am-241 and Cs-137. The LAC increased by 84% and 18% at gamma-ray energy of 0.059 and 0.662 MeV, when the PbO concentration raised between 5 and 20 wt%, respectively. Then the transmission rate and half-value layer of the fabricated composites were reduced by raising the PbO concentration. Therefore, the fabricated composite has good shielding properties in the low gamma-ray energy interval to be suitable for medical applications and low radioactive waste container constructions.

Keywords: epoxy resin, lead oxide, Sb_2O_3, NaI detector, radiation

*** Corresponding author: M. I. Sayyed,** Department of Physics, Faculty of Science, Isra University, Amman, Jordan; Department of Nuclear Medicine Research, Institute for Research and Medical, Consultations (IRMC), Imam Abdulrahman Bin Faisal University (IAU), P.O. Box 1982, Dammam, 31441, Saudi Arabia, e-mail: dr.mabualssayed@gmail.com
Aljawhara H. Almuqrin: Department of Physics, College of Science, Princess Nourah bint Abdulrahman University, P.O. Box 84428, Riyadh 11671, Saudi Arabia
Heba Jamal ALasali: Department of Physics, Faculty of Science, Isra University, Amman, Jordan
K. G. Mahmoud: Department of Nuclear Power Plants and Renewable Energy Sources, Ural Power Engineering Institute, Ural Federal University, st. Sofia Kovalevskoy, 5, 620002, Yekaterinburg, Russia

1 Introduction

It is imperative that any radiation that is produced by devices that continue to utilize the use of radiation be contained and prevented, to the greatest extent feasible, from reaching out to either people or the natural environment. Ionizing radiation can cause major health problems if it is exposed to it for an extended period of time, which is why radiological shields are commonly utilized to protect people from its potentially dangerous effects. Radiation shields are layers of substances that are positioned between a source of radiation and a target region to protect from radiation (1). Materials used for radiation shielding have been developed specifically to absorb the maximum amount of radiation that can be accommodated by the given setting. It may be necessary for a radiation shield to be lightweight, flexible, cheap, and eco-friendly and have the capacity to absorb radiation for very long periods, based on the particulars of the situation (2–10).

Epoxy resins are widely used as a foundational material for the fabrication of various composite materials. The exceptional performance of epoxy resins is well known. Epoxy resins provide a number of useful properties when correctly cured, such as cure in a vast range of temperature conditions, corrosion resistance, excellent capabilities in terms of electrical insulation and retention, high compression, tensile, and bending strengths, low cost, and low toxicity. When epoxy resins are mixed with other fillers, they produce composite materials that have features that are useful in a wide variety of applications. This is due to the fact that epoxy resins function effectively even when subjected to extreme conditions. Epoxy resin, when combined with heavy metal oxides, can be shaped into an effective shield of ionizing radiation (11–15). There have been many different ways explored to get a deeper understanding of the resistance of altered epoxy composites to ionizing radiation. In addition, a great deal of effort has been put into developing novel radiation-shielding

polymers that are based on epoxy and have a high level of functionality (16–19). One of the primary goals of nuclear engineers is to produce radioactive shielding materials using epoxy with high atomic number fillers like Pb, Sb, or W (20–23). These days, polymeric composites are effective, environmentally friendly materials with several uses in radiation protection equipment used in X-ray rooms, hospital computerized tomography (CT) rooms, and other settings. In addition, polymeric materials can be used in the construction of containers that are used in the transportation of low-level liquid radioactive wastes (LLW) and intermediate-level liquid radioactive wastes (ILWs) (24–27).

The most significant industrial antimony is produced in the antimony(III) oxide Sb_2O_3 compound. Sb_2O_3 is an important catalyst that is used in the vulcanization of rubber as well as the manufacturing of polyethylene terephthalate plastic. On the other hand, lead oxide is one of the main compounds that are preferable for radiation shielding applications due to its compactness and high density of lead (28). The walls, floors, and ceilings of the lab and consultation rooms were constructed using lead-lined plywood and lead-lined drywall. When there are cutouts or penetrations, lead angles are intended to offer leak-proof nuclear shielding (29). Furthermore, epoxy reinforced with PbO compounds is an eco-friendly material that does not produce any type of lead dust on the surface of fabricated materials. Lead dust has the main dangerous effect on human health because lead dust may become airborne and be inadvertently inhaled or ingested by humans (30).

Based on the effective gamma radiation shielding properties of PbO and Sb_2O_3, as well as the benefits of epoxy composites, such as their softness, easy fabrication, and excellent environmental adaptability, the current work novelty is to fabricate new composites based on inexpensive epoxy reinforced with Sb_2O_3/PbO to be utilized in radiation shielding applications. An experimental evaluation of the fabricated composites' gamma ray shielding capacity was performed in the low- and mid-gamma-ray energy intervals.

2 Materials and methods

This work used a two-component epoxy thermosetting resin: type A represents the epoxy resin, while type B is the hardener. The density of the pure epoxy resin used in this work is 1.1 $g{\cdot}cm^{-3}$ under a solidification time of 24 h. The utilized epoxy resin and curing agent utilized in the current work were supplied by SlabDOC (Ivanovo, Russia), where the epoxy resin and its curing agent were mixed in a ratio of 2:1. In addition, two different oxides, Sb_2O_3 (Fluka, purity >98%) and PbO (Sigma-Aldrich, purity >99%), were used as doping compounds to prepare the current radiation shielding materials. Four different sample compositions were formed by the molding and curing process. For all fabricated composites, the concentration of Sb_2O_3 was kept constant at 10 wt%, while the PbO compound was inserted at concentrations ranging from 5 to 20 wt%. After weighing the epoxy matrix, the required amount of PbO and Sb_2O_3 doping compounds are added. The mixture is mixed well under magnetic stirring for 15 min to ensure that the particles are evenly dispersed throughout the matrix. The mixture was thoroughly stirred before being put into a cylindrical mold with a diameter of 3 cm and a height of up to 3 cm. It was then left to freely set for 24 h without any outside interference before being removed from the mold (Figure 1). For each composite, four different thicknesses were fabricated to measure the radiation shielding parameters experimentally.

In order to determine the density of the newly developed Sb_2O_3/PbO-doped epoxy composites, the electric balance with an uncertainty of ±0.001 mg was used to measure the fabricated composites' mass in the air (W_{air}, g)

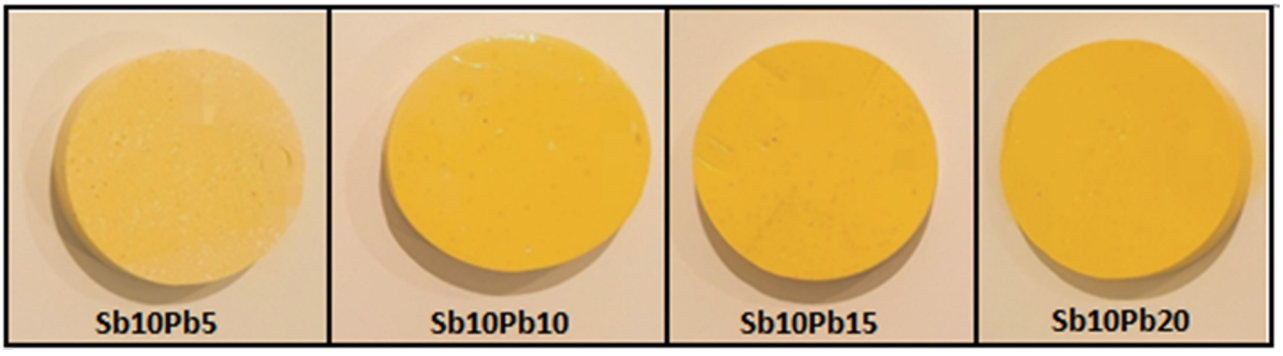

Figure 1: The prepared epoxy reinforced by Sb_2O_3/PbO composites.

Table 1: The composition of the newly developed composites

	Chemical composition (wt%)				
	Pure cured epoxy	**Sb10Pb5**	**Sb10Pb10**	**Sb10Pb15**	**Sb10Pb20**
H	6.97	5.91	5.56	5.20	4.85
C	43.89	37.32	35.09	32.87	30.66
Na	0.23	0.20	0.18	0.17	0.16
O	36.42	32.83	31.35	29.88	28.41
Na	2.35	1.98	1.87	1.75	1.63
Cl	8.47	7.19	6.76	6.33	5.90
K	1.50	1.27	1.19	1.12	1.04
Co	0.17	0.14	0.13	0.13	0.12
Sb	0.00	8.47	8.46	8.45	8.45
Pb	0.00	4.71	9.40	14.09	18.78
Density ($g{\cdot}cm^{-3}$)	1.03	1.30	1.35	1.40	1.49

and immersed in the ethanol (W_e, g). Then, the fabricated composites' density was measured by applying the Archimedes principle (Eq. 1) (31):

$$\rho = \frac{W_{air}}{W_{air} - W_e} \times \rho_e \tag{1}$$

In the above equation, ρ_e is 0.789 $g{\cdot}cm^{-3}$. The chemical composition and the density of the pure curing epoxy in addition to the fabricated composites are illustrated in Table 1.

A collimated gamma-ray method with the help of a NaI (Tl) detector was utilized to measure the linear attenuation coefficient (LAC). The NaI (Tl) crystal is a Harshaw type with dimensions 250 mm × 60 mm and can detect gamma-ray photons with energy intervals between 15 keV and 3 MeV. The NaI (Tl) resolution is less than 7.5% at 0.662 MeV. The NaI crystal was capsuled by an aluminum sheet with a thickness of 0.4 mm. The setup that was utilized for this study can be seen in Figure 2. Two radioactive sources Am-241 (with the energy of 0.059 MeV) and Cs-137 (with the energy of 0.662 MeV) were employed to measure the fabricated composites' LAC. The measurement was carried out both with and without a prepared composite, and the peak in the spectrum was identified with the use of the CASSY Lab 2. The radioactive source's activity concentration was determined in the presence (N) and absence (N_0) of the substance being tested (Figure 3), and as a result, the LAC was computed experimentally using the following formula (4,32–34):

$$\text{LAC} = \frac{1}{x}\text{In}\left(\frac{N_0}{N}\right) \tag{2}$$

where x (cm) represents the thickness of the fabricated composites. The thicknesses of the fabricated epoxy composites were measured using an X-PERT digital caliper

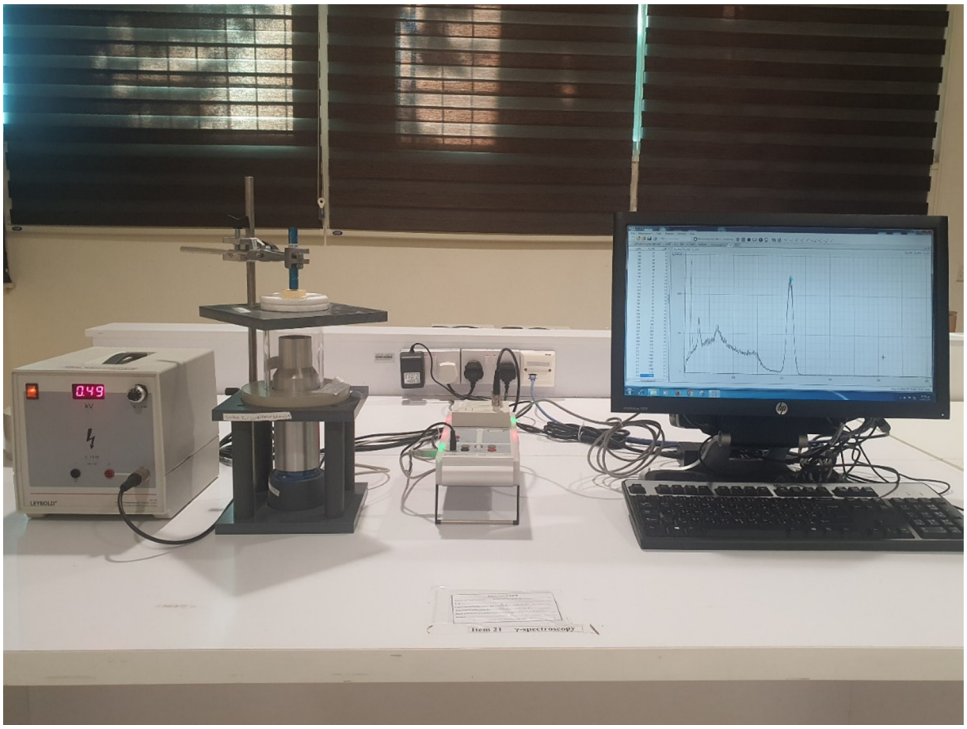

Figure 2: The experimental setup for the NaI (Tl) detector used to measure the attenuation factors of the current composites.

with measurement ranges of 0–150 mm (0–6 IN) and measurement uncertainty of 0.01 mm (0.0005 IN) produced in Moscow, Russia.

The transmission rate (TR), which is the ratio of the number of photons transmitted from the fabricated samples' thickness (N) to the total number of photons emitted from the radioactive source (N_o), can be described as follows (35,36):

$$\mathrm{TR} = \frac{N}{N_o} \tag{3}$$

Other shielding parameters, such as the half-value layer (HVL), mean free path, and tenth value layer (TVL), were estimated using the measured LAC data as follows (37–39):

$$\mathrm{HVL} = \frac{0.693}{\mathrm{LAC}} \tag{4}$$

$$\mathrm{MFP} = \frac{1}{\mathrm{LAC}} \tag{5}$$

$$\mathrm{TVL} = \frac{2.303}{\mathrm{LAC}} \tag{6}$$

3 Results and discussion

3.1 Density of the prepared samples

It is known that the density (ρ) is an important factor for the radiation shielding study, so we first examine the density of the new materials as a function of PbO content in Figure 4. It is reported that ρ lies within the range of 1.30–1.49 g·cm^{-3}, and this is higher than the pure epoxy, which is in the order of 1.1 g·cm^{-3}. The fabricated composites' ρ values increased with raising the PbO concentration from 5% to 20%, which is a logical finding since the amount of epoxy is decreased as we move from Sb10Pb5 to Sb10Pb20, while the amount of PbO is increased and it is known that the lead has a very high density, so we expected an enhancement in the density with increasing the content of PbO. However, the density of the manufactured composites was only increased by a factor of 14.6% when the PbO concentration was increased from 5 to 20 wt%.

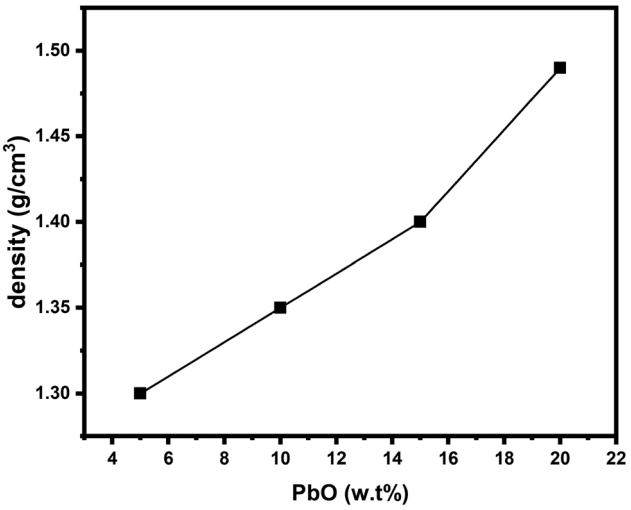

Figure 4: The influence of the fabricated composites' on the PbO concentration added to the fabricated composites.

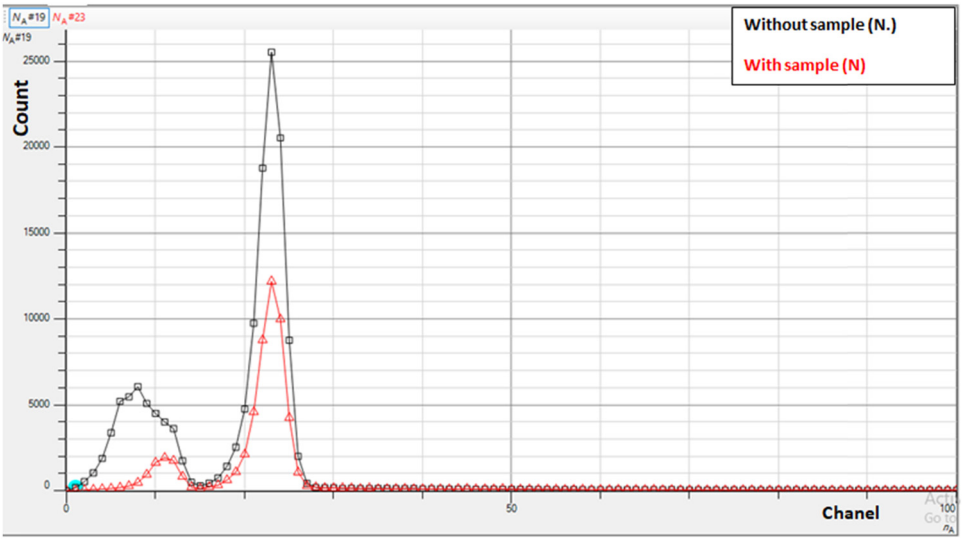

Figure 3: The experimental spectrum for Am-241 radioactive source measured by NaI (Tl) using CASSY Lab 2 software.

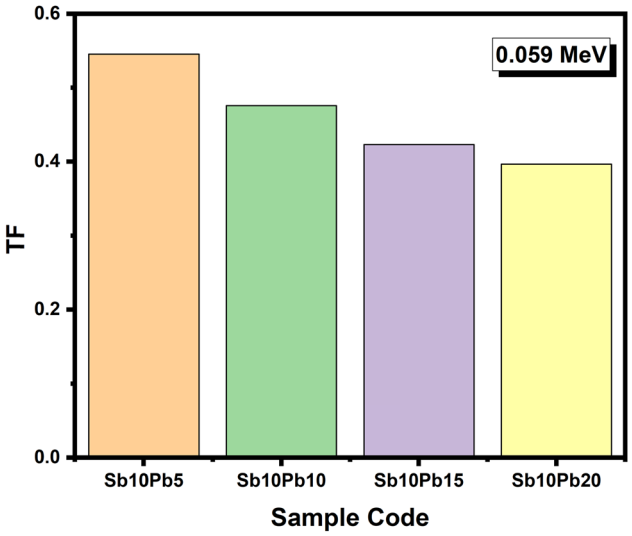

Figure 5: Dependence of the transmission rate TF vs the PbO insertion ratio in the fabricated composites.

3.2 Radiation shielding properties

The transmission ratio is affected by the enrichment of PbO concentration, where the enrichment of PbO content between 5 and 20 wt% significantly decreases the TF ratio from 0.55 to 0.4, respectively, at 0.059 MeV, as illustrated in Figure 5. The enrichment of PbO concentration in the fabricated composites increases the effective atomic number (Z_{eff}) and the interaction cross sections (electronic [σ_e] and atomic [σ_a]) as illustrated in Tables S1–S10. Therefore, the interactions between the incident photons and the electrons of the fabricated composites increased, followed by an increase in the amount of energy consumed inside the fabricated materials. As a result, the transposed photons do not have enough energy to penetrate the thickness of the fabricated composites and the TF values decreased. In addition, the TF results show an increase as energy is increased. The increase in gamma-ray energy is followed by a decrease in the interaction cross-sections, which causes a decrease in the number of interactions inside the fabricated composites. Therefore, the TF values increased as the incident gamma-ray energy increased.

Besides, LAC values were examined for the current composites-based epoxy with different contents of PbO at 0.059 and 0.662 MeV. Figure 6a illustrates that the LAC values were enhanced by 84% from 1.168 to 2.143 cm^{-1} by raising the PbO content from 5 to 20 wt%, respectively. The high enhancement is attributed to the cross-section of phonetic interaction (PE_{cs}), which changes with Z_{eff}^{4-5} in the low gamma-ray energy interval. Furthermore, increasing the incident gamma photon energy up to 0.662 MeV causes an increase in the Compton scattering interaction with a cross-section (CS_{cs}) that varies with Z_{eff} (40). Therefore, the enhancement in the LAC values was reduced to only 18% by raising the PbO concentration from 5 to 20 wt%, respectively (Figure 6b).

Figure 6a and b confirms a decrease in the LAC values as the incident gamma-ray energy increases. The decrease in LAC is attributed to the PE and CS interactions, which are prevalent interactions at low and intermediate gamma-ray energy. Moreover, the measured mass attenuation coefficient (MAC, $cm^2 \cdot g^{-1}$) for the fabricated composites

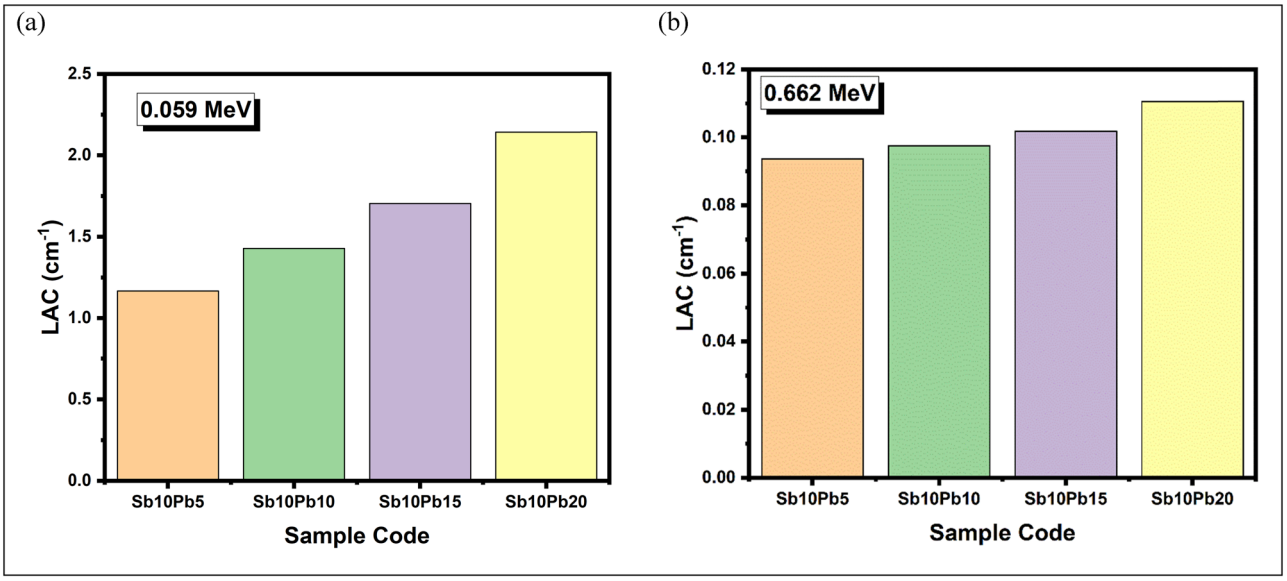

Figure 6: Variation of the LAC of the fabricated composites vs the PbO concentration at (a) 0.059 MeV and (b) 0.662 MeV.

Table 2: Comparison between the experimentally measured MAC and the theoretically calculated MAC using the Phy-X/PSD program

	MAC ($cm^2 \cdot g^{-1}$)					
	EXP	Phy-X	Diff (%)	EXP	Phy-X	Diff (%)
Sb10Pb5	0.8982	1.0293	12.7310	0.0721	0.0827	12.8914
Sb10Pb10	1.0591	1.2590	15.8778	0.0723	0.0842	14.0850
Sb10Pb15	1.2181	1.4880	18.1364	0.0728	0.0855	14.8400
Sb10Pb20	1.4387	1.7167	16.1947	0.0742	0.0868	14.4444

was compared to the theoretically calculated MAC (41) in Table 2 for energies 0.059 and 0.662 MeV. The comparison shows agreement between the experimental and theoretical calculations, with a difference ranging ±15%. The high difference is attributed to the uncertainty in the NaI (Tl) measurements as well as the uncertainty in thickness and chemical composition measurements.

In addition, the role of the incrementation of PbO contents on the half-value layer of the fabricated composites was studied at 0.059 and 0.662 MeV (Figure 7a and b). Figure 7a depicts a decrease in the HVL values from 0.593 to 0.323 cm, raising the PbO content between 5 and 20 wt%, respectively, at 0.059 MeV. The decrease in the HVL is related to the reverse proportionality between the HVL and the LAC values, where LAC = 0.693/LAC. At 0.059 MeV, the HVL considered for all composites is very small (<0.6 cm), which indicates that a thin layer of the prepared composites can be effectively developed to shield the low-energy radiation.

Figure 7b shows the dependence of the HVL values on the PbO concentration at 0.662 MeV. Unlike the HVL in the first case (i.e., 0.059 MeV), the HVL is relatively high at 0.662 MeV and spans from 6.26 to 7.39 cm. It means that a sample of the composite with a thickness of 6–7 cm is capable to lessen the intensity of half of the beam of the gamma-ray with an energy of 0.662 MeV. So, it is unsuitable to use epoxy resin samples that contain 10% Sb_2O_3 and different amounts of PbO (up to 20%) with a thickness smaller than 6 cm in applications that require attenuating photons with energies ≥0.662 MeV. In addition, from Figure 7b, we found that the HVL is maximum for Sb10Pb5 and minimum for Sb10Pb20, which again reaffirms the importance of using heavy metal oxide (PbO in our study) to improve the attenuation capabilities of the prepared composites.

In order to validate the fabricated composites, a comparison between the HVL of the current composites and the HVL of similar epoxy reinforced with some heavy metal oxide was performed and is presented in Figure 8a–d. At 0.662 MeV, Figure 8a shows a comparison of the HVL of the fabricated composites to the HVL of epoxy reinforced

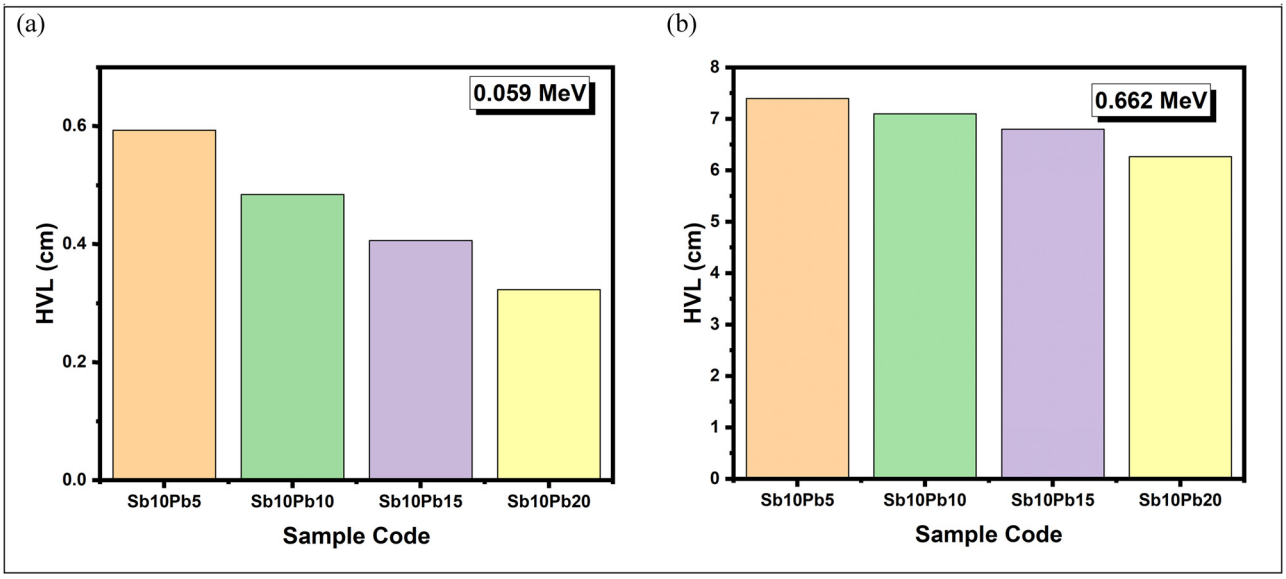

Figure 7: Variation of the HVL of the fabricated composites vs the PbO concentration at (a) 0.059 MeV and (b) 0.662 MeV.

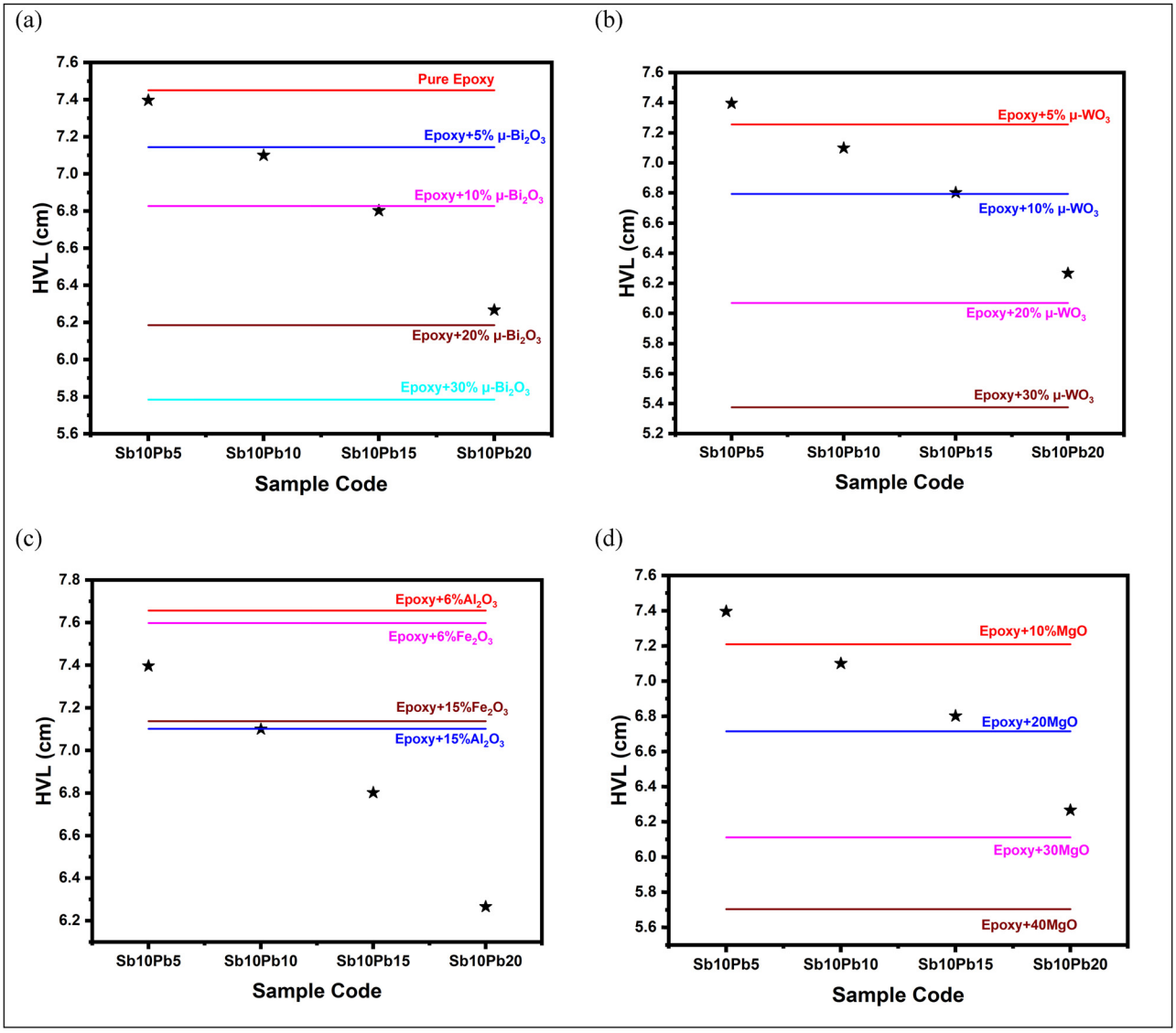

Figure 8: Comparison between the HVL of the current samples and the HVL of previously published epoxy reinforced with: (a) Bi_2O_3 compound, (b) WO_3 compound, (d) Al_2O_3 and Fe_2O_3 compounds, and (d) MgO compound.

by Bi_2O_3 compounds (42). The first observation from the data given in this figure is that the HVL for all the current epoxy composites and the epoxy-based micro Bi_2O_3 particles is lower than the HVL for the pure epoxy. This shows the importance of PbO or Bi_2O_3 in the radiation shielding field. On the other hand, Sb10Pb10 has an HVL close to that reported for the epoxy with 5% of Bi_2O_3. Moreover, Sb10Pb15 has an HVL close to that reported for the epoxy with 10% of Bi_2O_3, while Sb10Pb20 has an HVL slightly higher than that for the epoxy with 20% of Bi_2O_3.

Figure 8b shows a comparison of the fabricated composites' HVL to the HVL of the selected epoxy-based micro WO_3 particles (42). Obviously, the epoxy sample with 5% WO_3 has a higher HVL than Sb10Pb10 and a lower HVL than Sb10Pb5. Sb10Pb15 and epoxy with 10% of WO_3 have very close HVL. While, due to the high density of epoxy composites with 20% and 30% of Bi_2O_3, they have a lower HVL than all the prepared SbPb-composites.

In Figure 8c, epoxy composites with Al_2O_3 and Fe_2O_3 (14) were selected and the HVL for these composites with the HVL for the currently fabricated composites were compared. The prepared composites, Sb10Pb15 and Sb10Pb20, have much lower HVL than epoxy with Al_2O_3 and Fe_2O_3, thus they possess better attenuation competence. Sb10Pb10 has a very close HVL with an epoxy sample containing 15% Al_2O_3.

Figure 8d shows a comparison of the HVL of epoxy composites doped with various concentrations of micro-MgO

ranging from 10 to 40 wt% (11) with the currently fabricated composites HVL. The currently prepared composites, such as Sb10Pb20, have a much lower HVL than epoxy with 10% and 20% of MgO, while our SbPb-composites have a higher HVL than the epoxy with 30% and 40% of MgO.

4 Conclusion

Four different sample compositions containing Sb_2O_3 and PbO were formed by the molding and curing process. The experimental data show a rise in the LAC at 0.059 increased from 1.168 to 2.143 cm^{-1}. The aforementioned improvement is connected to a drop in the HVL values from 0.323 and 0.593 cm, enriching the PbO from 5 to 20 wt%, respectively. Increasing the energy to 0.662 MeV causes a decrease in the LAC associated with an increase in the HVL values, where the LAC enhanced by 18% is associated with a decrease in the HVL values from 6.26 and 7.39 cm, raising the PbO concentrations between 5 and 20 wt%, respectively, at 0.662 MeV. The enhancement in the LAC values is related to the reduction in the TF values, where the TF values were reduced from 0.55 to 0.40 by raising the PbO concentration between 5 and 20 wt%, respectively, at 0.059 keV. The fabricated epoxy-reinforced Sb_2O_3/PbO composites have a good shielding property at low- and mid-gamma-ray energy, but they are not effective to attenuate photons with energy higher than 0.662 MeV. Therefore, the fabricated new composites can be a suitable candidate for the construction of the LLW and ILW containers as well as for their efficient use in medical applications to shield the low and intermediate gamma-ray energetic photons.

Funding information: The authors express their gratitude to Princess Nourah bint Abdulrahman University Researchers Supporting Project number (PNURSP2023R2), Princess Nourah bint Abdulrahman University, Riyadh, Saudi Arabia.

Author contributions: Aljawhara H. Almuqrin: writing – review and editing, project administration; Heba Jamal ALasali: formal analysis, resources, methodology; M. I. Sayyed: writing – original draft, methodology; K. G. Mahmoud: visualization, writing – review and editing.

Conflict of interest: The authors state that there is no conflict of interest.

Data availability statement: All data generated or analyzed during this study are included in this published article (and its supplementary information files).

References

(1) Tishkevich DI, Grabchikov SS, Grabchikova EA, Vasin DS, Lastovskiy SB, Yakushevich AS, et al. Modeling of paths and energy losses of high-energy ions in single-layered and multilayered materials. IOP Conf Ser Mater Sci Eng. 2020;848:012089. doi: 10.1088/1757-899X/848/1/012089.

(2) More CV, Lokhande RM, Pawar PP. Effective atomic number and electron density of amino acids within the energy range of 0.122–1.330 MeV. Radiat Phys Chem. 2016;125:14–20. doi: 10.1016/j.radphyschem.2016.02.024.

(3) Vignesh S, Winowlin Jappes JT, Nagaveena S, Krishna Sharma R, Adam Khan M, More CV, et al. Development of lightweight polymer laminates for radiation shielding and electronics applications. Int J Polym Sci. 2022;2022:1–13. doi: 10.1155/2022/5252528.

(4) More CV, Bhosale RR, Pawar PP. Detection of new polymer materials as gamma-ray-shielding materials. Radiat Eff Defects Solids. 2017;172:469–84. doi: 10.1080/10420150.2017.1336765.

(5) Tishkevich DI, Grabchikov SS, Lastovskii SB, Trukhanov SV, Vasin DS, Zubar TI, et al. Function composites materials for shielding applications: Correlation between phase separation and attenuation properties. J Alloy Compd. 2019;771:238–45. doi: 10.1016/j.jallcom.2018.08.209.

(6) Dong M, Xue X, Yang H, Liu D, Wang C, Li Z. A novel comprehensive utilization of vanadium slag: As gamma ray shielding material. J Hazard Mater. 2016;318:751–7. doi: 10.1016/j.jhazmat.2016.06.012.

(7) Sayyed MI, El-Mesady IA, Abouhaswa AS, Askin A, Rammah YS. Comprehensive study on the structural, optical, physical and gamma photon shielding features of B_2O_3-Bi_2O_3-PbO-TiO_2 glasses using WinXCOM and Geant4 code. J Mol Struct. 2019;1197:656–65. doi: 10.1016/j.molstruc.2019.07.100.

(8) Dong M, Xue X, Yang H, Li Z. Highly cost-effective shielding composite made from vanadium slag and boron-rich slag and its properties. Radiat Phys Chem. 2017;141:239–44. doi: 10.1016/j.radphyschem.2017.07.023.

(9) Naseer KA, Sathiyapriya G, Marimuthu K, Piotrowski T, Alqahtani MS, Yousef ES. Optical, elastic, and neutron shielding studies of Nb_2O_5 varied Dy^{3+} doped barium-borate glasses. Opt (Stuttg). 2022;251:168436. doi: 10.1016/j.ijleo.2021.168436.

(10) Kamislioglu M. Research on the effects of bismuth borate glass system on nuclear radiation shielding parameters. Results Phys. 2021;22:103844. doi: 10.1016/j.rinp.2021.103844.

(11) Sayyed MI, Yasmin S, Almousa N, Elsafi M. Shielding properties of epoxy matrix composites reinforced with MgO micro- and nanoparticles. Materials. 2022;15:6201. doi: 10.3390/ma15186201.

(12) Elsafi M, Almousa N, Almasoud FI, Almurayshid M, Alyahyawi AR, Sayyed MI. A novel epoxy resin-based composite with zirconium and boron oxides: An investigation of photon attenuation. Cryst (Basel). 2022;12:1370. doi: 10.3390/cryst12101370.
(13) Zali VS, Jahanbakhsh O, Ahadzadeh I. Preparation and evaluation of gamma shielding properties of silicon-based composites doped with WO_3 micro- and nanoparticles. Radiat Phys Chem. 2022;197:110150. doi: 10.1016/j.radphyschem.2022.110150.
(14) Aldhuhaibat MJR, Amana MS, Jubier NJ, Salim AA. Improved gamma radiation shielding traits of epoxy composites: Evaluation of mass attenuation coefficient, effective atomic and electron number. Radiat Phys Chem. 2021;179:109183. doi: 10.1016/j.radphyschem.2020.109183.
(15) Alavian H, Samie A, Tavakoli-Anbaran H. Experimental and Monte Carlo investigations of gamma ray transmission and buildup factors for inorganic nanoparticle/epoxy composites. Radiat Phys Chem. 2020;174:108960. doi: 10.1016/j.radphyschem.2020.108960.
(16) Li J, Wu Z, Huang C, Li L. Gamma irradiation effects on cyanate ester/epoxy insulation materials for superconducting magnets. Fusion Eng Des. 2014;89:3112–6. doi: 10.1016/j.fusengdes.2014.09.012.
(17) Li R, Gu Y, Yang Z, Li M, Hou Y, Zhang Z. Gamma ray shielding property, shielding mechanism and predicting model of continuous basalt fiber reinforced polymer matrix composite containing functional filler. Mater Des. 2017;124:121–30. doi: 10.1016/j.matdes.2017.03.045.
(18) Liu Y, Liu B, Gu Y, Wang S, Li M. Gamma radiation shielding property of continuous fiber reinforced epoxy matrix composite containing functional filler using Monte Carlo simulation. Nucl Mater Energy. 2022;33:101246. doi: 10.1016/j.nme.2022.101246.
(19) Noor Azman NZ, Siddiqui SA, Low IM. Synthesis and characterization of epoxy composites filled with Pb, Bi or W compound for shielding of diagnostic X-rays. Appl Phys A. 2013;110:137–44. doi: 10.1007/s00339-012-7464-7.
(20) Oto B, Kavaz E, Durak H, Aras A, Madak Z. Effect of addition of molybdenum on photon and fast neutron radiation shielding properties in ceramics. Ceram Int. 2019;45:23681–89. doi: 10.1016/j.ceramint.2019.08.082.
(21) Gökçe HS, Öztürk BC, Çam NF, Andiç-Çakır Ö. Gamma-ray attenuation coefficients and transmission thickness of high consistency heavyweight concrete containing mineral admixture. Cem Concr Compos. 2018;92:56–69. doi: 10.1016/j.cemconcomp.2018.05.015.
(22) Kamislioglu M. An investigation into gamma radiation shielding parameters of the (Al:Si) and (Al + Na):Si-doped international simple glasses (ISG) used in nuclear waste management, deploying Phy-X/PSD and SRIM software. J Mater Sci Mater Electron. 2021;32:12690–704. doi: 10.1007/s10854-021-05904-8.
(23) Şensoy AT, Gökçe HS. Simulation and optimization of gamma-ray linear attenuation coefficients of barite concrete shields. Constr Build Mater. 2020;253:119218. doi: 10.1016/j.conbuildmat.2020.119218.
(24) Shin SH, Choi WN, Yoon S, Lee UJ, Park HM, Park SH, et al. Radiological analysis of transport and storage container for very low-level liquid radioactive waste. Nucl Eng Technol. 2021;53:4137–41. doi: 10.1016/j.net.2021.06.024.
(25) Tashlykov OL, Litovchenko Y, Vasutin NA, Sayyed MI, Khandaker MU, Mahmoud KA. Improvement in the design of shielding containers for intermediate-level radioactive waste. Radiat Phys Chem. 2022;200:110229. doi: 10.1016/j.radphyschem.2022.110229.
(26) Mahmoud KA, El-Soad AMA, Kovaleva EG, Almousa N, Sayyed MI, Tashlykov OL. Modeling a three-layer container based on halloysite nano-clay for radioactive waste disposal. Prog Nucl Energy. 2022;152:104379. doi: 10.1016/j.pnucene.2022.104379.
(27) Vujović M, Vujisić M. Applicability of polymer and composite inner linings in containers for borehole disposal of sealed radioactive sources – A simulation-based study of radiation effects. Prog Nucl Energy. 2021;137:103793. doi: 10.1016/j.pnucene.2021.103793.
(28) Mirji R, Lobo B. Radiation shielding materials: A brief review on methods, scope and significance; 2017. https://www.researchgate.net/publication/317687481.
(29) AbuAlRoos NJ, Baharul Amin NA, Zainon R. Conventional and new lead-free radiation shielding materials for radiation protection in nuclear medicine: A review. Radiat Phys Chem. 2019;165:108439. doi: 10.1016/j.radphyschem.2019.108439.
(30) Hulbert SM, Carlson KA. Is lead dust within nuclear medicine departments a hazard to pediatric patients? J Nucl Med Technol. 2009;37:170–2. doi: 10.2967/jnmt.109.062281.
(31) Aloraini DA, Almuqrin AH, Sayyed MI, Kumar A, Gaikwad DK, Tishkevich DI, et al. Experimental and theoretical analysis of radiation shielding properties of strontium-borate-tellurite glasses. Opt Mater (Amst). 2021;121:111589. doi: 10.1016/j.optmat.2021.111589.
(32) Liang S, Qin Y, Gao W, Wang M. A lightweight polyurethane-carbon microsphere composite foam for electromagnetic shielding. E-Polymers. 2022;22:223–33. doi: 10.1515/epoly-2022-0023.
(33) Gao L, Zhang J, Cui Y, Wang X. Effect of Zr-doped $CaCu_3Ti_{3.95}Zr_{0.05}O_{12}$ ceramic on the microstructure, dielectric properties, and electric field distribution of the LDPE composites. E-Polymers. 2023;23:20228100. doi: 10.1515/epoly-2022-8100.
(34) More C, Pawar P, Badawi M, Thabet A. Extensive theoretical study of gamma-ray shielding parameters using epoxy resin-metal chloride mixtures. Nucl Technol Radiat Prot. 2020;35:138–49. doi: 10.2298/NTRP2002138M.
(35) Mahmoud KA, Sayyed MI, Almuqrin AH, Elhelaly MA, Alhindawy IG. Synthesis of glass powders for radiation shielding applications based on zirconium minerals' leach liquor. Radiat Phys Chem. 2023;207:110867. doi: 10.1016/j.radphyschem.2023.110867.
(36) Alhindawy IG, Gamal H, Almuqrin AH, Sayyed MI, Mahmoud KA. Impacts of the calcination temperature on the structural and radiation shielding properties of the NASICON compound synthesized from zircon minerals. Nucl Eng Technol. 2023;55(5):1885–91. doi: 10.1016/j.net.2023.02.014.
(37) Aygün B. High alloyed new stainless steel shielding material for gamma and fast neutron radiation. Nucl Eng Technol. 2020;52:647–53. doi: 10.1016/j.net.2019.08.017.
(38) Saleh A. Comparative shielding features for X/Gamma-rays, fast and thermal neutrons of some gadolinium silicoborate

glasses. Prog Nucl Energy. 2022;154:104482. doi: 10.1016/j.pnucene.2022.104482.
(39) Aygün B. Neutron and gamma radiation shielding properties of high-temperature-resistant heavy concretes including chromite and wolframite. J Radiat Res Appl Sci. 2019;12:352–9. doi: 10.1080/16878507.2019.1672312.
(40) Mahmoud KG, Sayyed MI, Almuqrin AH, Arayro J, Maghrbi Y. Monte Carlo investigation of gamma radiation shielding features for Bi_2O_3/epoxy composites. Appl Sci. 2023;13:1757. doi: 10.3390/app13031757.
(41) Erdem Ş, Özgür F, Al B, Sayyed MI, Kurudirek M. Phy-X/PSD: Development of a user friendly online software for calculation of parameters relevant to radiation shielding and dosimetry. Radiat Phys Chem. 2020;166. doi: 10.1016/j.radphyschem.2019.108496.
(42) Karabul Y, İçelli O. The assessment of usage of epoxy based micro and nano-structured composites enriched with Bi_2O_3 and WO_3 particles for radiation shielding. Results Phys. 2021;26:104423. doi: 10.1016/j.rinp.2021.104423.